

Meso-scopic deformation in brittle granular materials

William D Neal^{1,2}, Gareth J Appleby-Thomas³ and Gareth S Collins²

¹ Institute of Shock Physics, Imperial College London, SW7 2AZ, UK

² Applied Modelling and Computational Group, Imperial College London, SW7 2AZ, UK

³ Dynamic Response Group, Cranfield University, Shrivenham, UK

E-mail: will.neal@awe.co.uk

Abstract. Compaction is the process of removing void-space from a porous material. In brittle particulate systems, the majority of densification is caused by particle fracture. This preliminary study aimed to investigate the differences in fracture behaviour between quasi-statically and shock loaded glass-microsphere beds. Macro-scale quasi-static ($20 \mu\text{m s}^{-1}$) and dynamic compaction curves were measured that show subtle qualitative differences in stress-density space. Samples were recovered from a quasi-static and dynamic experiment at a similar order of stress. Differences in fracture behaviour were observed that may explain the differences in crush curves. Results suggest that the primary *total-fracture* process occurs relatively instantaneously at low stresses in the quasi-static regime. The sphere fracture process is slow relative to the stress-wave therefore causing a different fracture pattern in the shock regime.

1. Introduction

Particulate materials are ideally suited to shock absorbing applications due to the large amount of energy required to deform their inherently complex meso-structure in the process of compaction. Significant effort is being made to improve macro-scale compaction models to represent these important, but complex, materials. On the long road towards achieving this capability, an important milestone would be to understand how particle deformation mechanisms are affected by loading rate.

It has been suggested that the inter-particle fracture process can be divided into three different fracture mechanisms: *total-fracture*, *abrasion* and *attrition* [1]. A macro-scale particulate compaction event may include any of these processes but their relative importance is likely controlled by the rate at which the system is compacted.

It is often convenient and cost-effective to approximate a material's stress-density shock-compaction response by quasi-static data. However, this may not be appropriate due to the presence of mechanisms that are inhibited or enhanced by dynamic loading. It has therefore been suggested that compaction mechanisms can be divided into regimes: *quasi-static* and *dynamic-only* [2]. An early investigation into how brittle particulate materials compact should, therefore, first discover if there are any significant particle deformation mechanisms that only occur in the dynamic loading regime.



2. Methodology

Compaction experiments were conducted in the quasi-static and shock loading regimes. Figure 1 (a) shows the quasi-static compaction assembly based on the design used in [3]. A sample of soda-lime glass microspheres (particle size $180 - 212 \mu\text{m}$, described further in [4]) were positioned between steel punches of diameter $10.000 \pm 0.001 \text{ mm}$. The sample was compressed using an Instron 600KPX universal testing machine at 0.02 mm s^{-1} and the resulting axial force (F_{Total}) was measured to an uncertainty of $\pm 1 \%$ at a frequency of 10 Hz up to 1400 kN.

A maraging-steel annulus confined the sample radially. A piezo-resistive strain gauge was positioned on the outer surface of the annulus to measure hoop strain of the radially expanding steel. The hoop strain was used to calculate radial strain within the sample and therefore improve the accuracy of the sample volume change.

A linear variable differential transformer (LVDT) measured the displacement of the upper punch to $\pm 0.02 \text{ mm}$ thus allowing the change in sample volume to be calculated. A load cell was placed between the annulus and the lower machine platen to measure the force transmitted through friction ($F_{Friction}$) between the sample and the walls of the annulus. Therefore the stress transmitted by the sample (σ_x) and the compaction density (ρ) could be calculated using the methodology used in [3].

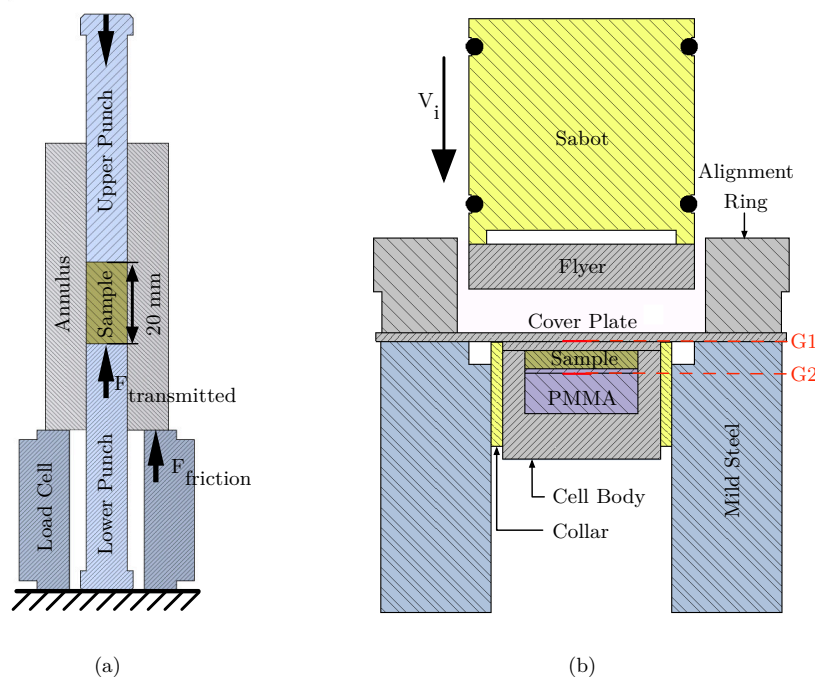


Figure 1. Experimental apparatus (a) the quasi-static compaction assembly showing forces within the assembly and (b) shock assembly showing a flyer plate impact.

A single shock recovery experiment was conducted on a single-stage light gas-gun using the assembly shown in figure 1 (b). The assembly allowed the microsphere sample to experience a single shock-wave transmission followed by a longitudinal release caused by the rear of the flyer plate without being affected by lateral releases from the edge of the container/flyer-plate. The $3.70 \pm 0.01 \text{ mm}$ thick microsphere sample was contained within an aluminium container. The mass of the sample and volume of the container was used to calculate the initial density of the microsphere bed ($\rho_{00} = 1.50 \pm 0.05 \text{ g cm}^{-3}$). An aluminium (1050) flyer plate impacted

an aluminium (2014-T6511) cover plate at $0.58 \pm 0.07 \text{ mm } \mu\text{s}^{-1}$. Adhered to the rear of the cover-plate was the sample recovery cell. The adhesive layer contained a manganin piezoresistive gauge (LM-SS-125CH-048) to measure the wave profile as it entered the recovery cell. This layer also provided a convenient spall plane for the recovery container to separate from the 4 kg steel momentum trap present to slow the projectile. A second manganin gauge, positioned within the PMMA buffer plate measured the wave profile transmitted by the sample (G2).

The time between the two shock-waves recorded by G1 and G2 was used to calculate the shock velocity within the sample ($U_s = 1.60 \pm 0.02 \text{ mm } \mu\text{s}^{-1}$) in the same manner as [4]. The shock velocity was then used to infer the particle velocity (u_p) within the sample using the previously measured Hugoniot relationship:

$$U_s = C_0 + S u_p = 0.41 + 1.86 u_p \quad (1)$$

$$u_p = \frac{U_s - C_0}{S} = 0.64 \text{ mm } \mu\text{s}^{-1} \quad (2)$$

The Hugoniot stress could then be calculated using the following jump condition:

$$P = \rho_0 U_s u_p = 1.8 \pm 0.3 \text{ GPa} \quad (3)$$

Subsamples of the recovered microspheres from the quasi-static and shock compaction experiments were imaged using a Scanning Electron Microscope (SEM). A surface of an adhesive, conducting tape was dipped into the microsphere subsample. The sample was coated with approximately 10 nm of gold to improve electrical conduction. This single layer of particles or agglomerated particles was then imaged.

The remainder of the compacted sample was suspended in water and agitated with a small propeller for approximately one minute to allow agglomerated particles to separate. The suspension was then analysed with a Mastersizer 2000 laser diffraction particle size analyser. The laser diffraction method measures particle volume and infers diameter on the assumption that each particle is a sphere. This approach was not necessarily quantitatively accurate due to this assumption but provided a good qualitative description of the range of particle sizes.

3. Results and discussion

The quasi-static stress-density curve is plotted in figure 2 along with the shock compaction data previously measured in [4]. The agreement between the curves are good although there are subtle differences in shape and magnitude.

The high stress response of the quasi-static sample appears to deviate from the shock-compaction curve. It is possible that this deviation represents a transition from a quasi-static particle-deformation mechanism to a dynamic one but more likely a failure in the shock-compaction data fit. From the limited number of shock-compaction measurements, it is not possible to conclude that any difference occurred in this region with any certainty.

The quasi-static compaction curve shows a similar transition in the stress-density history at σ_p (see figure 2) as the shock-compaction states deduced from the precursor wave feature in [4]. The magnitude of this stress is significantly lower in the quasi-static regime which suggests this is likely a property of the material that is affected by loading-rate.

Figure 4 shows a SEM image from a microsphere sample quasi-statically loaded to a longitudinal stresses of 1.12 GPa. The image shows a fractured sphere amongst fragments from other fractured spheres within the bed. The surface fractures appear to initiate from an indentation caused by contact from a neighbouring sphere. The number of sphere fragments is high compared to the number of fragments observed in the shock-loaded sample in figure 5. There was no visible indentation in the sphere in the shock loaded subsample (or other spheres within the sample) which may suggest that the sphere was fractured during the passage of the

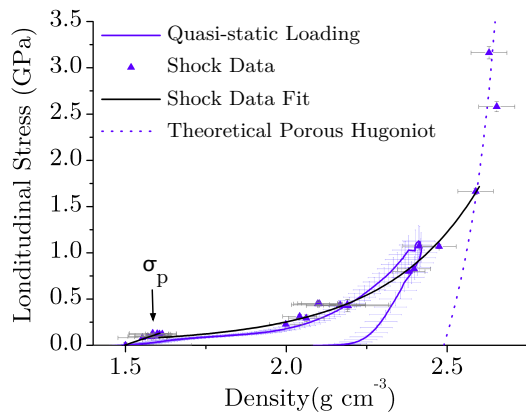


Figure 2. Quasi-static and shock compaction curves showing data from [4]. Theoretical porous Hugoniot calculated with method from [5].

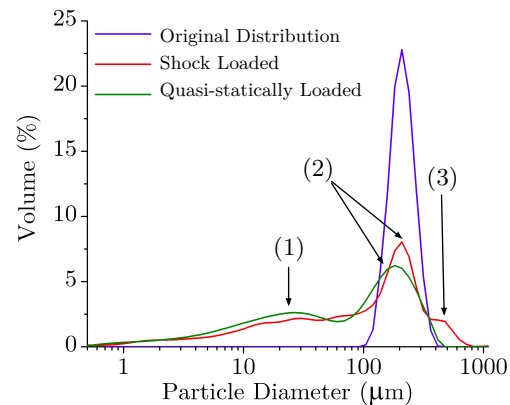


Figure 3. Laser diffraction particle-size analysis data from original and recovered samples after compaction showing features of distribution (1, 2 & 3).

shock-wave rather than the stress concentrations caused by the collision of neighbouring spheres. The shock front thickness calculated by the method in [4] shows the macro-scale shock front thickness is on the order of 2 particles. This suggests the spheres are fractured during the shock transition of the spheres as there is little time for neighbouring spheres to cause a stress concentration from their contact.

The surrounding fragments appear so be of similar size in each loading regime. In both regimes, the primary fracture mechanism is *total-fracture* in the first instance but it is possible that *abrasion* and *attrition* mechanisms contribute to the comminution of these larger fragments in the shock regime.

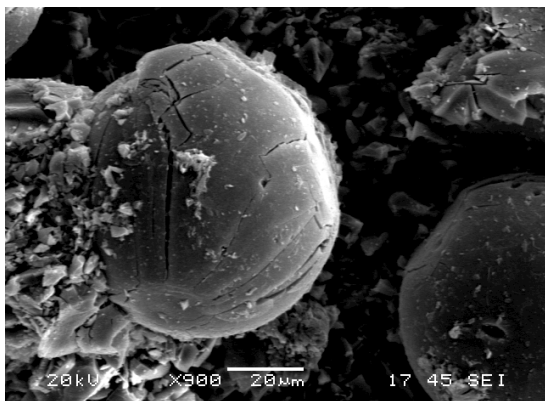


Figure 4. SEM image from a recovered microsphere sample after **quasi-static** loading to $\sigma_x = 1.12$ GPa.

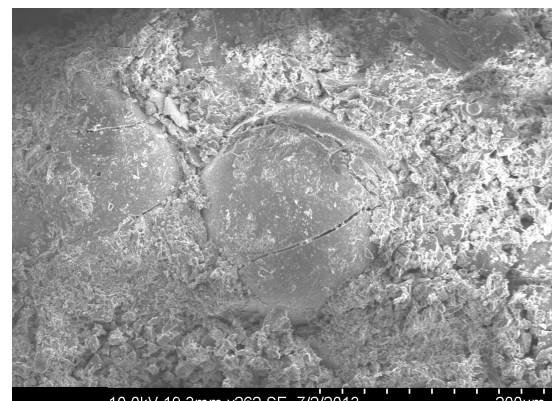


Figure 5. SEM image from a recovered microsphere sample after **shock** loading to $\sigma_x = 1.79$ GPa.

The particle size analysis measurements of the recovered samples are shown in figure 3 along with the distribution of the original material. The modal peak (2) of the two recovered samples is consistent with the original sample showing a significant number of spheres that did not undergo fracture in any way. The volume of the modal peak is larger in the shock recovered

sample compared to the quasi-static sample despite the shock loaded sample undergoing a higher stress and densification. Therefore, in the dynamic regime, there were fewer fractured spheres at a similar applied stress.

It is likely that the secondary peak (1) in the quasi-statically loaded distribution occurs from the similar size fragments produced from the initial sphere total-fracture. This peak is not so pronounced in the shock loaded distribution indicating that a broader range of fragment sizes is produced in this regime. This is consistent with the qualitatively different fracture pattern observed in figures 4 and 5 and suggests the agrees with the possibility of abrasion and attrition fracture mechanisms occurring in this regime.

An increase in particle size in the shock loaded sample is evident from figure 3 where the size distribution of the recovered sample exceeds the original distribution (point 3). This suggests that particle agglomeration is more prevalent under dynamic loading than in the quasi-statically loaded samples. Although agglomeration of particles and fragments was observed in the quasi-static samples, it is possible that agitation during the particle size analysis method was sufficient to break apart these agglomerates in the quasi-statically loaded sample but not in the shock loaded sample. Therefore, it appears that particles were more effectively bonded together by the shock compaction process compared to the quasi-static.

4. Conclusions

The stress-density compaction curves appear qualitatively similar, under quasi-static and shock loading, for the 180 - 212 μm soda-lime glass microspheres chosen for this experiment. They are therefore a good approximation for each other in this particular material. There are subtle differences that seem to be related to differing particle deformation mechanisms prevalent under the differing loading rates.

In the quasi-static regime particles fracture as a result of stress concentrations caused by neighbouring particles. This process produces a secondary peak in the particle size distribution that was not observed in the shock-loaded sample. SEM images suggest that under quasi-static loading smaller, similar-sized fragments are produced therefore dissipating large amounts of fracture energy in during the initial sphere total-fracture. A similar image of the shock induced fracture process shows larger fragments were produced by the initial sphere fracture. The similarity in particle-size distributions conclude that the shock compaction process also potentially included abrasion and attrition fracture mechanisms after this initial sphere fracture which indicates a relatively large amount of the fracture energy is dissipated at a later stage in the shock compaction process compared to the quasi-static compaction process.

The similarities in the stress-density compaction response between the two loading rates requires further investigation that must include some form of meso-scopic fracture-sensitive numerical simulations. It is unlikely that further experimental recovery can explain the time-dependant particle deformation involved in the shock compaction of this system but it is clear that the fracture patterns are different from in both regimes.

Acknowledgements

The Institute of Shock Physics acknowledges the support of AWE and Imperial College London.

References

- [1] Cooper W and Breaux B 2010 *Int J Fracture* **162** 137–150
- [2] Benson D, Nesterenko V, Jonsdottir F and Meyers M 1997 *J Mech Phys Solids* **45** 1955–1999
- [3] Vogler T, Lee M and Grady D 2007 *Int J Solids Struct* **44** 636–658
- [4] Neal W, Chapman D and Proud W 2011 *AIP Conf. Proc* **1426** 1443–1446
- [5] Meyers M A Dynamic behaviour of materials, 1994 *John Wiley & Sons*